Ordering and director-field configuration in single droplets of liquid crystals probed by X-ray microdiffraction

EUROPHYSICS LETTERS 15 July 2002

Europhys. Lett., **59** (2), pp. 218–224 (2002)

Ordering and director-field configuration in single droplets of liquid crystals probed by X-ray microdiffraction

O. Francescangeli[1], C. Ferrero[2], L. Lucchetti[1], F. Simoni[1] and M. Burghammer[2]

[1] *Dipartimento di Fisica e Ingegneria dei Materiali e del Territorio and INFM Università di Ancona - Via Brecce Bianche, I-60131 Ancona, Italy*

[2] *European Synchrotron Radiation Facility - Boîte Postale 220 F-38043 Grenoble Cedex, France*

(received 7 February 2002; accepted in final form 11 April 2002)

PACS. 61.30.Cz – Molecular and microscopic models and theories of liquid crystal structure.
PACS. 07.85.Qe – Synchrotron radiation instrumentation.
PACS. 61.10.Eq – X-ray scattering (including small-angle scattering).

Abstract. – X-ray microdiffraction (μ-XRD) is used for the first time to probe the liquid crystal (LC) ordering in confined LCs. We report on the direct observation of the director field in single droplets of nematic LCs embedded in a solid polymeric matrix (polymer-dispersed LCs). The bipolar configuration is identified in droplets with radius $R \leq 1\,\mu$m. Both the director distribution function and the droplet order parameter are obtained from diffraction patterns and the results are in excellent agreement with theoretical calculations. This technique is unique in its application to dispersed mesophases in that it allows to probe the local (μm length scale) LC ordering. The possibility of focusing measurements on single droplets eliminates the problems connected with averaging, which are typical of other techniques. Our results prove that μ-XRD is a novel and valuable tool in the study of confined LCs and open new exciting opportunities for future investigations.

Liquid crystals (LCs) confined to curved geometries have intrigued scientists for many years because of their important role in emerging technologies and the large variety of physical phenomena they exhibit. Interest in this field has expanded greatly after the discovery of polymer-dispersed liquid crystals (PDLCs) in the mid-1980s. PDLCs are composite materials consisting of spherical droplets of low molar mass LCs, randomly dispersed in a polymeric matrix [1]. The droplet sizes may vary from the submicrometer region up to tens of microns, with droplets in the range 1–5 μm being the most common. Beyond the scope of applications [2], the interest in PDLCs has considerably stimulated fundamental research, concerning the phase separation and polymerization process [3], the optical properties [4, 5], and especially the effects which are due to the confinement of LCs to small cavities [6]. In this case, a variety of unusual effects are introduced due to the large surface-to-volume ratio. The most observable are changes in the nature of the phase transitions and the specific director configuration.

Understanding the details of the nematic-director configuration within droplets is of paramount importance in the study of PDLCs. When the droplet sizes are of the order of a few microns, the critical interplay between the ordering interactions at the boundary surface and the strong elastic deformation energies inside the volume results in a rich variety of director configurations [1]. External fields and temperature changes can be used to induce transitions from one configuration to another, and these transitions can be used to obtain a measure of the surface anchoring strength [7]. The primary experimental tools used so far to determine the nematic configuration within LC droplets have been optical polarizing microscopy and magnetic resonance spectroscopy. The former is easy to perform but is limited to droplet sizes greater than a few microns. ^{2}H-NMR is a powerful mean to probe LC systems not amenable to optical microscopy [8], however, specially deuterated nematic probe molecules must be used and only average information over a large number of cavities is obtained. In addition, a droplet radius $R < 0.5\,\mu$m is requested in order to prevent significant distortion by the magnetic field.

The aim of the present paper is to demonstrate the effectiveness of X-ray microdiffraction (μ-XRD) as a new experimental tool to probe LC ordering and director-field configuration within *single* droplets of PDLCs. To this purpose, a micro-focused X-ray beam is used in transmission geometry and diffraction patterns from single droplets of an ultrathin-layer PDLC sample are collected and analysed. As very distinctive patterns can be observed corresponding to different configurations, this technique provides a unique tool to investigate the dependence of both LC ordering and director configuration on the droplet shape and size.

The samples were prepared via thermally initiated *Polymerization Induced Phase Separation* (PIPS) starting from a mixture of the epoxy resins EPON815 (by Shell, 25.4% in weight) and MK107 (by Wilmington, 7.1%) with the hardener Capcure 3-800 (by Miller Stephenson, 32.5%) and the nematic LC E7 (by Merck, 35%; $T_{\mathrm{KN}} = 263\,\mathrm{K}$, $T_{\mathrm{NI}} = 334\,\mathrm{K}$). This mixture is known to form LC droplets with the *bipolar* configuration [1, 6, 9, 10]. This is the preferred configuration in the case of strong parallel molecular anchoring and single-elastic-constant approximation; the director field has cylindrical symmetry with the symmetry axis defined by two surface-point defects lying at the opposite ends of the droplet surface [11]. Ultrathin films of the PDLC samples were sliced out by means of a liquid-nitrogen–refrigerated microtome. The thickness of the film ($5\,\mu$m) was chosen to be comparable with the droplet size in order to reduce the probability for the probing X-ray beam to cross more than one droplet. Scanning Electron Microscopy (SEM) analysis of a section of the investigated sample revealed a narrow distribution of spherical droplet sizes with an average droplet diameter of $2.0 \pm 0.1\,\mu$m. The diffraction experiments were carried out using the SAXS/WAXS scanning microdiffraction setup of the ID13 microfocus beamline [12] at the ESRF (Grenoble, France). A monochromatic beam ($\lambda = 0.784\,$Å or $\lambda = 1.109\,$Å) of $2\,\mu$m diameter ($2\,\mu$rad divergence) produced by a tapered-glass capillary X-ray optics was used. The PDLC film sample (S) was supported by an electron microscopy copper grid which was mounted on a high-resolution ($< 1\,\mu$m) translation stage. A CCD microscope was used to select areas of interest on the sample. The data were collected at room temperature ($T = 297\,\mathrm{K}$). Two-dimensional (2D) diffraction patterns were recorded using a 130 mm MarCCD detector (D; pixel size $64.45\,\mu$m). The S-D distance was 109.08 mm. The resolution in the scattering angle was $\Delta(2\theta) = 3 \cdot 10^{-2}$ degrees. The selected region was mapped in steps of $2\,\mu$m in both the horizontal and vertical directions. Different areas of the sample were investigated.

μ-XRD measurements on thin films of samples after removing the LC by evaporation (under vacuum) confirmed the amorphous nature of the polymer matrix. Only after prolonged annealing at room temperature, effects of local partial ordering of the polymer chains were detected. As the polymer matrix is amorphous and isotropic (at least on the micrometer length

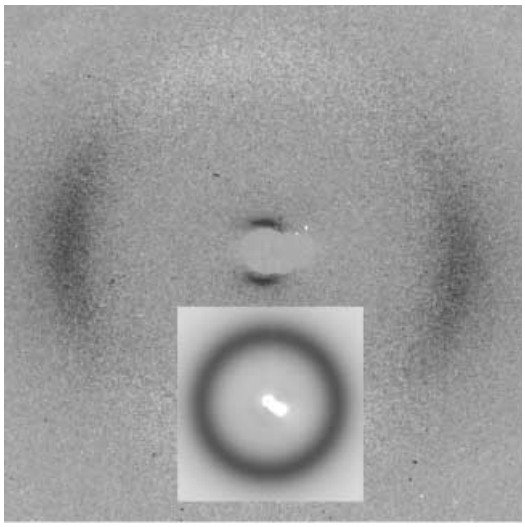

Fig. 1

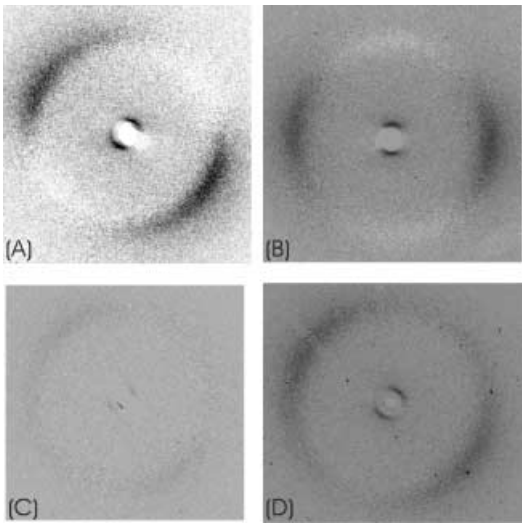

Fig. 2

Fig. 1 – XRD pattern ($\lambda = 0.784\,\text{Å}$) of a single spherical droplet of a $5\,\mu$m thick PDLC film measured with the microfocus ($2\,\mu\text{m} \times 2\,\mu\text{m}$) beam line ID13 at the ESRF. The droplet radius is $R \leq 1\,\mu$m. The inset shows the μ-XRD pattern of the polymer matrix bulk surrounding the LC droplet.

Fig. 2 – Examples of XRD patterns of single bipolar droplets showing different orientations of the droplet axis. In all cases the droplet radius is less than $1\,\mu$m. (A-C): $\lambda = 0.784\,\text{Å}$; (D): $\lambda = 1.109\,\text{Å}$. The pattern in (D) was taken after submitting the sample to a thermal cycle.

scale), whereas bipolar droplets possess LC ordering and anisotropic director configuration, we could discriminate between the scattering from a droplet and that from the polymer binder in all cases except when the droplet axis was parallel to the incident beam. For the LC droplets we observed anisotropic patterns featured by a weak small-angle diffuse peak characteristic of the short-range nematic positional order, whereas for the polymer matrix we observed isotropic patterns without any small-angle signal. In principle, the appearance of the small-angle peak is subject to the proper orientation of the droplet axis relative to the incident beam. However, the relatively wide orientational distribution function of the nematic domains around the symmetry axis in the bipolar droplets allowed us to observe this peak essentially in all cases except when the droplet axis direction was parallel (or very close) to the direction of the incident beam. SEM analysis [13] confirmed the correspondence between anisotropic pattern and LC droplet.

Figure 1 reports a representative example of the μ-XRD pattern of a single LC droplet. This pattern was obtained from the measured one after subtracting the contribution of the isotropic background due to the polymeric matrix surrounding the selected droplet (inset of fig. 1). The diameter of this droplet was estimated to be less than $2\,\mu$m because no LC contribution to the scattered intensity was observed in the nearest-neighbours sampling points. The anisotropy of the pattern is associated with a director-field configuration possessing cylindrical symmetry and is similar to the typical diffraction patterns observed for axially oriented nematics [14]. The preferred orientation axis, $\boldsymbol{N}$, is given by the straight line through the small-angle peaks (*i.e.* the meridional line). The symmetry of this pattern around the equator ensures that the droplet axis lies in (or very close to) the plane orthogonal to the incident

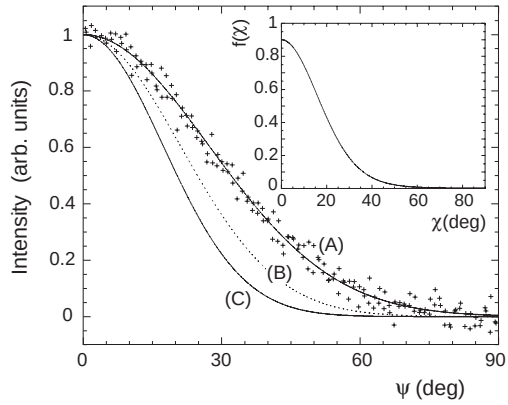

Fig. 3 – (A) Azimuthal intensity profile (at constant $q = 1.4\,\text{Å}^{-1}$) of the wide-angle diffuse crescents of the μ-XRD pattern of fig. 1: symbols represent the experimental data whereas the full thin line gives the best fit by a Gaussian lineshape. (B) Theoretical azimuthal intensity profile that should be obtained with $\boldsymbol{n}$ parallel to $\boldsymbol{N}$ everywhere within the droplet. (C) Deconvolution of curves (A) and (B). All the curves are normalized to their maximum value. The inset shows the orientational distribution function of the nematic director inside the bipolar droplet.

beam. Other examples of μ-XRD patterns of single spherical droplets are reported in fig. 2 where different orientations of the droplet axis are shown. The weak scattering signal in (C) is due to a submicrometer droplet; measurements of relative intensity allowed us to estimate a radius $R \leq 0.3\,\mu$m. The pattern of fig. 2(D) was taken after submitting the sample to a thermal cycle through the clearing point, in order to eliminate possible effects of the slicing process on the LC orientation. No significant difference is observed in this pattern compared to the others.

The dominant feature of the scattering (fig. 1) for $\boldsymbol{q} \| \boldsymbol{N}$ ($q = 4\pi \sin\theta/\lambda$) is the pair of small-angle diffuse peaks centered at $q = 0.218\,\text{Å}^{-1}$ arising from longitudinal correlations in the molecular arrangement and corresponding to a spacing $d = 2\pi/q = 28.8\,\text{Å}$. The two wide-angle diffuse crescents centered on the equatorial line ($\boldsymbol{q} \perp \boldsymbol{N}$) at $q \cong 1.4\,\text{Å}^{-1}$ are associated to the short-range liquid-like positional order of the molecules and correspond to an average molecular distance $d \cong 4.5\,\text{Å}$. However, differently from what observed for perfect axially aligned samples, distinct arc-shaped profiles of both meridional and equatorial reflections are clearly evident in the diffraction pattern, indicating a distribution of angular orientations of the coherently scattering domains relative to the average $\boldsymbol{N}$. Such a distribution reflects the curvature of the nematic director-field lines inside the bipolar droplet.

The azimuthal intensity profile (at $q = 1.4\,\text{Å}^{-1}$) of the wide-angle diffuse crescents is shown in fig. 3. By analyzing this profile we have obtained the distribution function of the nematic director in the droplet and determined the droplet order parameter S_D. This represents the first experimental determination of such important quantities. The concept of droplet order parameter was introduced by Kelly and Palffy-Muhoray [5] within a model formulated to describe the electro-optical response of PDLCs. The nematic within a droplet is assumed to possess a local director configuration $\boldsymbol{n}(\boldsymbol{r})$ and order parameter $S(\boldsymbol{r})$. From this assumption a droplet director $\boldsymbol{N}_\text{D}$ and droplet order parameter S_D are defined representing the average orientation of the nematic:

$$S_\text{D} = \left\langle \left\{ 3\left[\boldsymbol{N}_\text{D} \cdot \boldsymbol{n}(\boldsymbol{r})\right]^2 - 1 \right\} / 2 \right\rangle_{V_\text{D}} = \left\langle P_2\left(\boldsymbol{N}_\text{D} \cdot \boldsymbol{n}(\boldsymbol{r})\right) \right\rangle_{V_\text{D}}, \tag{1}$$

where $P_2(\boldsymbol{N}_\mathrm{D} \cdot \boldsymbol{n}(\boldsymbol{r}))$ is the second-order Legendre polynomial and the average is calculated over the droplet volume V_D. $\boldsymbol{N}_\mathrm{D}$ is parallel to the average orientation of the local director $\boldsymbol{n}(\boldsymbol{r})$ within the droplet and for the bipolar configuration it coincides with the symmetry axis $\boldsymbol{N}$. In the following we describe the guidelines of the approach used to determine S_D; the details will be reported in a forthcoming paper [13].

The azimuthal spread of the equatorial diffuse peaks results from two different causes: one is the curvature of the director-field lines inside the droplet and the other one is the thermal orientational disorder of the molecules that results in a distribution of molecular orientations around the local average direction $\boldsymbol{n}(\boldsymbol{r})$. The latter contribution is always present, even for an ideal uniform configuration with $\boldsymbol{n}$ parallel to $\boldsymbol{N}$ at each point in the sample volume (*i.e.*, $S_\mathrm{D} = 1$). In that case the azimuthal intensity profile at constant q, $I_0(\psi)$, is related to the orientational distribution function of the molecules, $f(\beta)$, as follows [15]:

$$I_0(\psi) = \int_{\beta=\psi}^{\pi/2} f(\beta) \sec^2 \psi \big(\tan^2 \beta - \tan^2 \psi \big)^{-1/2} \sin \beta \, \mathrm{d}\beta, \tag{2}$$

where the azimuth ψ is measured relative to the equatorial axis and the distribution function $f(\beta)$ is defined such that $2\pi f(\beta) \sin \beta \, \mathrm{d}\beta$ gives the fraction of molecules that have their long axes at an angle between β and $\beta + \mathrm{d}\beta$ with respect to the director $\boldsymbol{n}$.

For a general configuration with curved director-field lines, the contribution of elementary domains having different average orientation $\boldsymbol{n}$ must be considered. If $G(\alpha) \, \mathrm{d}\alpha$ is the fraction of the droplet volume where $\boldsymbol{n}$ is oriented at an angle between α and $\alpha + \mathrm{d}\alpha$ with respect to $\boldsymbol{N}$, then its contribution to the scattered intensity is given by $\mathrm{d}I = I_0(\psi - \alpha) G(\alpha) \, \mathrm{d}\alpha$. Assuming that the LC order parameter S is not appreciably affected by the confinement and is constant everywhere within the droplet, the azimuthal spread of the intensity profile can be expressed through the convolution integral

$$I(\psi) = \int_0^\pi I_0(\psi - \alpha) G(\alpha) \, \mathrm{d}\alpha, \tag{3}$$

where $I_0(\psi)$ is given by eq. (2). This approximation is reasonable for supramicron-sized droplets far from the N-I transition temperature because the length scale over which the droplet surface affects the local nematic order (*i.e.* tens of nanometers) is small compared to the droplet radius [16, 17]. Following the procedure described in ref. [15], $G(\alpha)$ can be expressed [13] by means of an equation that is formally equivalent to eq. (2):

$$G(\alpha) = C \int_{\chi=\alpha}^{\pi/2} f_\mathrm{D}(\chi) \sec^2 \alpha \big(\tan^2 \chi - \tan^2 \alpha \big)^{-1/2} \sin \chi \, \mathrm{d}\chi, \tag{4}$$

where $f_\mathrm{D}(\chi)$ is the orientational distribution function of the nematic director inside the droplet (χ is the angle between $\boldsymbol{n}$ and $\boldsymbol{N}$) and C is a proportionality constant. The function $f_\mathrm{D}(\chi)$ is characteristic of the director configuration and its determination allows calculation of S_D through eq. (1), *i.e.* $S_\mathrm{D} = \int_0^\pi P_2(\cos\chi) f_\mathrm{D}(\chi) \sin\chi \, \mathrm{d}\chi / \int_0^\pi f_\mathrm{D}(\chi) \sin\chi \, \mathrm{d}\chi$. The function $G(\alpha)$ was obtained by deconvolution of the experimental profile $I(\psi)$ with the function $I_0(\psi)$ representing the intrinsic spreading associated to the thermal molecular disorder. This required first a model to calculate $I_0(\psi)$. In the nematic phase $f(\beta)$ conforms closely [14, 15] to the simple Maier-Saupe mean-field distribution [18]; accordingly, we assumed $f(\beta) = \exp[m \cos^2 \beta]/4\pi Z$, where Z is a normalization constant and $m = 3(US/k_\mathrm{B}T)/2$, U being the orientational potential energy function. The room-temperature value of m was determined by imposing that the nematic order parameter $S = \langle 3\cos^2\beta - 1 \rangle / 2$ equals the value 0.6 experimentally measured

in bulk nematic $E7$ at the same temperature [19]; this gave the value $m = 4.45$. Numerical integration of eq. (2) allowed us to calculate $I_0(\psi)$ and the result is shown in fig. 3 (dotted line B). In the same figure the function $G(\psi)$ resulting from the numerical deconvolution of $I(\psi)$ and $I_0(\psi)$ is also reported (full line C). Finally, by numerical inversion of the integral equation (2) we obtained the droplet director distribution function $f_{\mathrm{D}}(\chi)$ shown in the inset of fig. 3. The droplet order parameter was then calculated by means of eq. (1) and the result obtained was $S_{\mathrm{D}} = 0.73$, with an estimated [13] error of ± 0.02. This value is in excellent agreement with theoretical calculations of S_{D} for bipolar droplets [5, 9, 13] and with data of optical phase shift measured in similar PDLC samples [10]. In particular, if the director field is modelled by assuming that the local director is oriented along a series of elliptical lines lying on a series of nested ellipsoids [20], the calculated [13] value of S_{D} is 0.70. If the small difference between experimental and theoretical value of S_{D} is significant, it can be attributed either to slight imperfections in the spherical shape of the droplets or to a small deviation from the condition of strong surface anchoring. In the latter case, such difference could be used to get quantitative information of the anchoring energy [13], which has never been measured so far for these systems.

An analysis similar to that described above can be extended to other configurations and used to discriminate among configurations showing the same cylindrical symmetry but differing in the director orientational distribution function, as is the case for the bipolar and axial ones [1, 13].

From the radial intensity profile of the small-angle reflections, the longitudinal (*i.e.* parallel to $\boldsymbol{n}$) correlation length, $\xi_{\parallel}$, in the confined nematic phase has been calculated. This quantity measures the length scale over which correlations of molecular positions vanish and characterizes the short-range positional order of the nematic phase. The best fit to the experimental profile was obtained with a Lorentzian lineshape centered at $q_0 = 0.218\,\text{Å}^{-1}$ with a full width at half-maximum (FWHM) $\Delta q = 3.44 \cdot 10^{-2}\,\text{Å}^{-1}$ corresponding to the correlation length $\xi_{\parallel} = 2/\Delta q = 58\,\text{Å}$. This value is about a factor three the correlation length $\xi_{\parallel} \cong 20\,\text{Å}$ measured in bulk nematic $E7$. An increase of the apparent molecular length, $d = 2\pi/q_0$, from the value $d_{\mathrm{B}} \cong 26.5\,\text{Å}$ in bulk nematic to the actual $d = 28.8\,\text{Å}$ must also be pointed out. The two effects have to be ascribed to the confinement of the LC, however, the most obvious interpretation in terms of an increase of the bulk orientational order parameter S cannot be proposed because the droplet radius is much larger than the typical lengths over which surface interfacial interactions affect the local orientational order [16, 17]. A more detailed discussion of this point is beyond the scope of the present paper and will be reported elsewhere [13].

In conclusion, the presented results have proved the effectiveness of μ-XRD as a tool for studying LC ordering and director configuration in micron-sized confined geometries. For larger geometries, μ-XRD offers the unique possibility of probing the spatial dependence of LC ordering and average director orientation on the micrometer length scale. Further investigations regarding temperature and external field effects on LC order and phase behavior, as well as the smectic order evolution of smectogenic LCs in PDLCs are planned. This technique opens new opportunities in the quantitative study of translational ordering of LCs in the presence of induced disorder as in highly porous solids or randomly interconnected network of pores [6]. Improving the spatial resolution by reducing the beam size would allow experiments on smaller volumes (or smaller portions of the same confined system), thus disclosing several new studies, including the probing of mesophase/substrate interactions and the influence of segregation on the local order parameter. The possibility of performing μ-XRD experiments on weakly scattering samples with submicron-sized beam (at least in one dimension) has recently been shown [21] using a $3 \times 0.1\,\mu\text{m}^2$ beam. Basing upon the present experience, the limiting factor when moving down to smaller beam dimensions seems to be

radiation damage (for most organic samples) rather than low flux density. Single photon counting detectors with low dark current and low readout noise in connection with further efforts in background reduction (*e.g.*, helium environment, smaller beamstops) will help to push the size limits even more down.

REFERENCES

[1] Drzaic P. S., *Liquid Crystal Dispersions* (World Scientific, Singapore) 1995.
[2] Simoni F. and Francescangeli O., *Intern. J. Polym. Mater.*, **45** (2000) 381.
[3] Lucchetti L. and Simoni F., *J. Appl. Phys.*, **88** (2000) 3934.
[4] Khoo I. C. and Wu S.-T., in *Optics and Nonlinear Optics of Liquid Crystals* (World Scientific, Singapore) 1993, Chapt. 2.
[5] Kelly J. R. and Palffy-Muhoray P., *Mol. Cryst. Liq. Cryst.*, **243** (1994) 11.
[6] Crawford G. P. and Zumer S., in *Liquid Crystals in Complex Geometries*, edited by Crawford G. P. and Zumer S. (Taylor & Francis, London) 1995, Chapt. 1, and references therein.
[7] Erdmann J. H. *et al.*, *Phys. Rev. Lett.*, **64** (1990) 1907.
[8] Golemme A. *et al.*, *Phys. Rev. A*, **37** (1988) 559.
[9] Palffy-Muhoray P. *et al.*, *Mol. Cryst. Liq. Cryst.*, **179** (1990) 445.
[10] Basile F. *et al.*, *Phys. Rev. E*, **48** (1993) 432.
[11] Dubois-Violette E. and Parodi R., *J. Phys. (Paris) Coll. C*, **4** (1969) 57.
[12] Müller M. *et al.*, *Nucl. Instrum. Methods A*, **467-468** (2001) 958.
[13] Francescangeli O. *et al.*, in preparation.
[14] Leadbetter A. J., in *The Molecular Physics of Liquid Crystals*, edited by Luckhurst G. R. and Gray G. W. (Academic Press, London) 1979, Chapt. 13.
[15] Leadbetter A. J. and Norris E. K., *Mol. Phys.*, **38** (1979) 669.
[16] Vilfan I. *et al.*, *Phys. Rev. A*, **40** (1989) 4724.
[17] Kralj S. *et al.*, *Phys. Rev. A*, **43** (1991) 2943.
[18] De Gennes P. G. and Prost J., in *The Physics of Liquid Crystals* (Clarendon Press, Oxford) 1993.
[19] Hallam B. T. *et al.*, *J. Appl. Phys.*, **86** (1999) 6682.
[20] Williams R. D., *J. Phys. A*, **19** (1986) 3211.
[21] Müller M. *et al.*, *J. Appl. Crystallogr.*, **33** (2000) 1231.